ChemComm

Cite this: *Chem. Commun.*, 2011, **47**, 5235–5237

www.rsc.org/chemcomm

COMMUNICATION

Functionalized carbon nanomaterials as nanocarriers for loading and delivery of a poorly water-soluble anticancer drug: a comparative study†

Nanda Gopal Sahoo,[a] Hongqian Bao,[a] Yongzheng Pan,[a] Mintu Pal,[a] Mitali Kakran,[a] Henry Kuo Feng Cheng,[a] Lin Li*[a] and Lay Poh Tan[b]

Received 5th January 2011, Accepted 14th March 2011
DOI: 10.1039/c1cc00075f

Carbon nanomaterials such as multiwalled carbon nanotubes (MWCNTs) and graphene oxide (GO) have been functionalized by highly hydrophilic and biocompatible poly(vinyl alcohol) (PVA) for loading and delivery of an anticancer drug, camptothecin (CPT). For the first time, CPT was loaded onto MWCNT–PVA and GO–PVA through π–π interactions and its capability to kill human breast and skin cancer cells was investigated.

Carbon nanotubes (CNTs) and graphene have attracted tremendous attention as the most promising carbon nanomaterials in the 21st century for a variety of applications such as electronics,[1,2] biomedical engineering,[3–5] tissue engineering,[6] neuroengineering,[7] gene therapy,[8,9] and biosensor technology.[10,11] For the biomedical applications, CNTs have been utilized over existing drug delivery vectors due to their ability to cross cell membranes easily and their high aspect ratio as well as high surface area, which provides multiple attachment sites for drug targeting. However, the cytotoxicity of CNTs is controversial due to the use of CNTs with or without surface functionalization and the residual heavy metals in CNTs. The designed functionalized CNTs are biocompatible and do not have residual heavy metals. Therefore, they are expected to be nontoxic at the cellular level. Many groups have shown that the designed functionalized CNTs are able to reduce cytotoxic effects,[12,13] and at the same time improve biocompatibility,[14,15] thus, offering the potential exploitation of nanotubes for drug administration. On the other hand, more recently graphene and its derivatives have been enormously investigated in the biological applications because of their biocompatibility, unique conjugated structure, relatively low cost and availability on both sides of a single sheet for drug binding.[16,17]

Different approaches have been applied in order to load drug molecules to the sidewalls of functionalized CNTs and graphenes by covalent or noncovalent attachment.[18–20] Liu *et al*. utilized PEGylated nanoscale graphene oxide (NGO) as a nanocarrier to load anticancer drugs *via* noncovalent interaction and studied its cellular uptake.[21] Ali-Boucetta *et al*. investigated the noncovalent interaction of an anticancer drug, doxorubicin, with CNTs and evaluated its cytotoxic activity.[22] These works demonstrated that GO derivatives and CNTs can be used as efficient nanocarriers for loading and delivering water-insoluble aromatic drugs. However, the cellular uptake and cytotoxicity of a poorly water-soluble drug, camptothecin (CPT), when loaded onto both CNTs and GO as drug carriers, have not been investigated.

In this communication, we have functionalized multiwalled carbon nanotubes (MWCNTs) and graphene oxide (GO) with highly hydrophilic and biocompatible poly(vinyl alcohol) (PVA) in order to increase their aqueous solubility. We have used the PVA functionalized MWCNTs and GO to load and deliver CPT, while similar works have not been found in the literature. We have investigated the drug loading capacity and the cytotoxic activity of CPT-loaded CNT- and GO-based nanocarriers, and compared the efficiencies of these nanocarries for the first time. More importantly, by varying the grafted hydrophilic polymers, the strategy of attaching various insoluble, aromatic drugs onto functionalized CNTs and graphenes to discover more suitable nanocarriers can motivate further and extensive research.

MWCNT–COOH was prepared by the oxidation of raw MWCNTs with concentrated H_2SO_4/HNO_3 (volumetric ratio 3 : 1),[23] whereas GO was synthesized from natural graphite powder using a modified Hummers method.[24] The MWCNT–COOH and GO were further functionalized with PVA in a carbodiimide-activated esterification reaction (ESI†, Scheme S1). The functionalization of PVA on the MWCNTs and GO was confirmed by FTIR (ESI†, Fig. S1), TEM and AFM measurements (Fig. 1).

The TEM image (Fig. 1b) showed that the surface of a MWCNT has been covered by soft material which is believed to be PVA and also MWCNT–PVA was thicker than MWCNT–COOH (Fig. 1b). As shown in Fig. 1d and e, the GO existed as micron-sized platelets, whereas the GO–PVA sheets were 100–200 nm due to the repeated sonication during the synthesis procedures. The GO sheets had a thickness of about 0.8–1 nm with very sharp edges and a flat surface. In contrast, the thickness of GO–PVA was increased to ~2–3 nm and the edges of GO–PVA appeared to be relatively coarse

[a] *School of Mechanical and Aerospace Engineering, Nanyang Technological University, 50 Nanyang Avenue, 639798, Singapore. E-mail: mlli@ntu.edu.sg*
[b] *School of Materials Science and Engineering, Nanyang Technological University, 50 Nanyang Avenue, 639798, Singapore*

† Electronic supplementary information (ESI) available: Detailed experimental procedures and characterization data including FTIR, UV and cell viability. See DOI: 10.1039/c1cc00075f

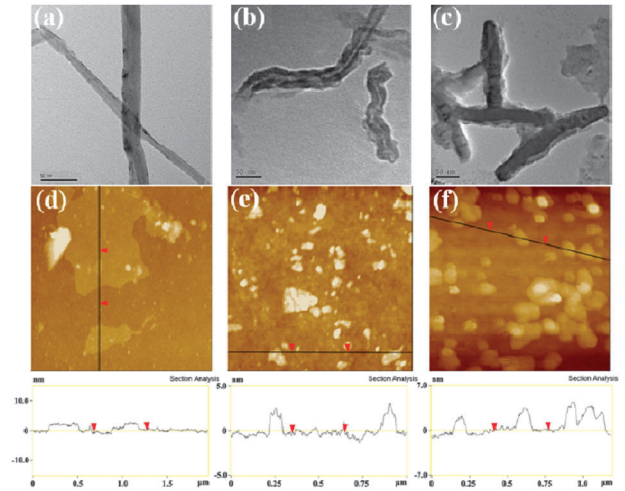

Fig. 1 TEM images of (a) MWCNT–COOH, (b) MWCNT–PVA, and (c) MWCNT–PVA–CPT; AFM images of (d) GO, (e) GO–PVA and (f) GO–PVA–CPT.

and some protuberances were seen on the surfaces, which were formed by wrapping and folding of PVA chains on the surface.

Next we studied the drug loading and binding of CPT to MWCNT–PVA and GO–PVA. In this research, we chose CPT as a model drug because it is widely used in clinics for cancer treatment. At first, the successful loading of the drug was achieved by simple mixing of a CPT–DMSO solution with an aqueous solution of MWCNT–PVA or GO–PVA (ESI†, Experimental). Any unbound or undissolved drug was removed by centrifugation and filtration, and dialysis was also used to remove any residual free CPT and DMSO. The UV-vis spectra of the resulting product were recorded to determine the loading efficiency of CPT on the MWCNT–PVA or GO–PVA. The amount of loaded drug was calculated by its absorption at 369 nm (after subtracting the absorption contribution from nanocarriers) with a molar extinction coefficient of 19 900 L mol^{-1} cm^{-1}(shown in Fig. 2b and ESI†, Fig. S2b).

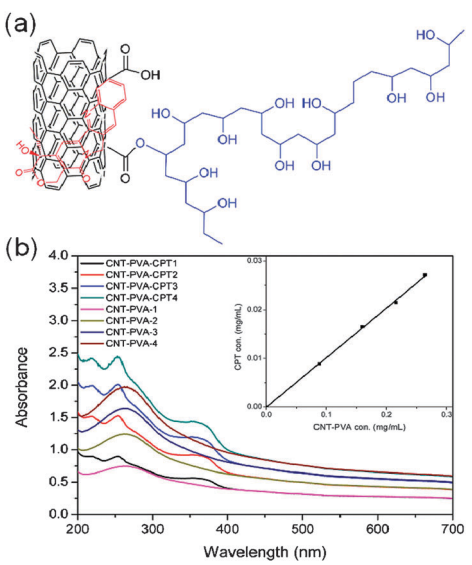

Fig. 2 CPT loading on MWCNT–PVA: (a) schematic depiction of CPT loaded MWCNT–PVA, and (b) UV spectra of MWCNT–PVA and MWCNT–PVA–CPT with different concentrations.

It was estimated that 1 g of MWCNT–PVA was able to load about 0.1 g of CPT, whereas 1 g of GO–PVA loaded 0.12 g of CPT. The *in vitro* release profiles of CPT from carriers in PBS buffer at 37 °C are summarized in Fig. S3, ESI†, and the accumulative plateau values of *ca.* 17.8–20.1% CPT release were reached upon 72 h, which suggested the strong hydrophobic interactions and π–π stacking between CPT and MWCNT or GO sheets (Fig. 2a, ESI†, Fig. S2a).[21,22] The small difference in the loading and retaining capacity of the drug between two kinds of nanocarriers is attributed to their similar chemical structures, and thus the close interactions with the MWCNT and GO. The binding of CPT was also confirmed by TEM and AFM measurements of MWCNT–PVA–CPT and GO–PVA–CPT, respectively (Fig. 1c and f). The TEM image of MWCNT–PVA–CPT clearly showed that the MWCNT cavities were blocked by CPT clusters, while the AFM image of MWCNT–PVA–CPT showed that the sheet thickness increased (~3–5 nm) after CPT loading.

Next we investigated the *in vitro* cytotoxic activity of these MWCNT–PVA–CPT and GO–PVA–CPT complexes using the MDA-MB-231 human breast cancer cells. The cells were incubated at 37 °C for 48 h with various concentrations of MWCNT–PVA–CPT, GO–PVA–CPT, MWCNT–PVA, GO–PVA and free CPT respectively. Free CPT was dissolved in DMSO and diluted in PBS. The relative cell viability was then measured by the standard MTT assay.[25,26] Several groups have used this assay to assess the cytotoxic response of cell cultures to carbon nanotubes and GO.[22,27,28] As shown in Fig. 3b, there is no obvious toxicity (>80% cell viability) measured for pure MWCNT–PVA and GO–PVA, even at a high concentration of 500 mg L^{-1} for MDA-MB-231 cells, revealing that the nanocarriers alone are not cytotoxic and the enhanced efficacy should be attributed to the contribution of the drug bound on them.

The cytotoxic activities of the water soluble MWCNT–PVA–CPT and GO–PVA–CPT complexes were significantly higher than that of the CPT alone. For example, MWCNT–PVA–CPT and GO–PVA–CPT complexes exhibited the more than 50% growth inhibition concentration (IC50) of about 400 nM and 700 nM, respectively, which were 15 and 8.5 folds more potent than free CPT dissolved in DMSO. The high potencies of MWCNT–PVA–CPT and GO–PVA–CPT complexes were also observed with other metastatic skin tumor cell lines (A-5RT3) (ESI†, Fig. S4). These results suggested that the MWCNT–PVA and GO–PVA can mediate the delivery of CPT and hence, enhance the cellular uptake of the drug. It also indicates that both MWCNT and GO have more available surface area for π–π interactions with the aromatic ring of CPT, which led to the enhanced cell killing efficiency. It is also observed from Fig. 3 that the MWCNT–PVA–CPT has a slightly higher cytotoxic efficiency than the GO–PVA–CPT at the same conditions, as confirmed from two cancer cells studies *in vitro*. We believe that the enhancement of *in vitro* cytotoxic efficiency was caused by CNT's high aspect ratio as well as high surface area, which provides multiple adherent styles to cells, leading to effective cell killing. Although significant progress has been made in understanding how CNTs cross the cell membrane, the

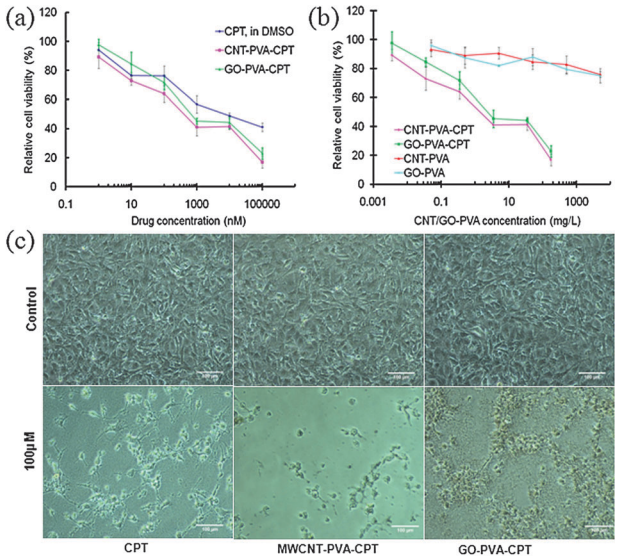

Fig. 3 (a) Relative cell viability of MDA-MB-231 cells cultured with free CPT, MWCNT–PVA–CPT and GO–PVA–CPT at different concentrations of CPT, respectively; (b) relative cell viability of MDA-MB-231 cells cultured with MWCNT–PVA and GO–PVA in the presence of and the absence of CPT, respectively; (c) optical images of MDA-MB-231 cells after culturing with CPT, MWCNT–PVA–CPT and GO–PVA–CPT, respectively.

proposed mechanisms are still being debated. To date, two major intracellular uptake mechanisms have been proposed: (1) endocytosis/phagocytosis and (2) nanopenetration. Wu *et al.*[18] and Cai *et al.*[29] reported that the CNTs are able to enter the cells by a nanopenetration mechanism, whereas other groups adopted the endocytosis mechanism for the cellular uptake of CNTs.[8,30,31] In the case of GO, Liu *et al.*[21] and Zhang *et al.*[20] suggested that the functionalized GO enters cells through the endocytosis mechanism. By comparing these works in the literature and our results, we can deduce that GO–PVA entered the cells through the endocytosis mechanism only, whereas MWCNT–PVA entered the cells likely through both nanopenetration and endocytosis mechanisms, which resulted in the relatively higher cytotoxic effect of MWCNT–PVA–CPT. However, further investigations are necessary to quantitatively understand the exact contributions from two pathways in this respect.

In summary, we have successfully synthesized MWCNT–PVA and GO–PVA and studied their application to the drug loading and cytotoxic activity of the drug, CPT. MWCNT–PVA and GO–PVA could form stable complexes with the CPT *via* noncovalent interactions. We have also shown that MWCNT–PVA–CPT and GO–PVA–CPT exhibited higher cytotoxic activity compared to free CPT alone, which was more evident in the case of MWCNT–PVA–CPT. Although GO sheets are recently reported as promising materials for drug delivery due to their surface availability on both sides for drug binding, we have interestingly found that the cytotoxic activity of MWCNT–PVA–CPT was superior to that of GO–PVA–CPT.

Authors acknowledge the financial support from Lee Kuan Yew Postdoctoral Fellowship and SUG grant M58050023, NTU, Singapore.

Notes and references

1 P. R. Bandaru, *J. Nanosci. Nanotechnol.*, 2007, **7**, 1239.
2 Y. Cao, S. Liu, Q. Shen, K. Yan, P. J. Li, J. Xu, D. P. Yu, M. L. Steigerwald, C. Nuckolls, Z. F. Liu and X. F. Guo, *Adv. Funct. Mater.*, 2009, **19**, 2743.
3 A. Bianco, K. Kostarelos, C. D. Partidos and M. Prato, *Chem. Commun.*, 2005, 571.
4 Z. Liu, J. T. Robinson, X. M. Sun and H. J. Dai, *J. Am. Chem. Soc.*, 2008, **130**, 10876.
5 K. Balasubramanian and M. Burghard, *Small*, 2005, **1**, 180.
6 B. S. Harrison and A. Atala, *Biomaterials*, 2007, **28**, 344.
7 E. B. Malarkey and V. Parpura, *Neurodegener. Dis.*, 2007, **4**, 292.
8 N. W. S. Kam, Z. Liu and H. Dai, *Angew. Chem., Int. Ed.*, 2006, **45**, 577.
9 R. Yang, X. Yang, Z. Zhang, Y. Zhang, S. Wang, Z. Cai, Y. Jia, Y. Ma, C. Zheng, Y. Lu, R. Roden and Y. Chen, *Gene Ther.*, 2006, **13**, 1714.
10 G. Cheng, J. Zhao, Y. Tu, P. He and Y. Fang, *Anal. Chim. Acta*, 2005, **533**, 11.
11 V. Dua, S. P. Surwade, S. Ammu, S. R. Agnihotra, S. Jain, K. E. Roberts, S. Park, R. S. Ruoff and S. K. Manohar, *Angew. Chem., Int. Ed.*, 2010, **49**, 2154.
12 C. P. Firme III and P. R. Bandaru, *Nanomedicine: NBM*, 2010, **6**, 245.
13 H. Dumortier, S. Lacotte, G. Pastorin, R. Marega, W. Wu, D. Bonifazi, J. P. Briand, M. Prato, S. Muller and A. Bianco, *Nano Lett.*, 2006, **6**, 1522.
14 A. Nimmagadda, K. Thurston, M. U. Nollert and P. S. McFetridge, *J. Biomed. Mater. Res., Part A*, 2006, **76A**, 614.
15 S. Murugesan, T.-J. Park, H. Yang, S. Mousa and R. J. Linhardt, *Langmuir*, 2006, **22**, 3461.
16 S. Park, N. Mohanty, J. W. Suk, A. Nagaraja, J. H. An, R. D. Piner, W. W. Cai, D. R. Dreyer, V. Berry and R. S. Ruoff, *Adv. Mater.*, 2010, **22**, 1736.
17 Y. B. Zhang, S. F. Ali, E. Dervishi, Y. Xu, Z. R. Li, D. Casciano and A. S. Biris, *ACS Nano*, 2010, **4**, 3181.
18 W. Wu, S. Wieckowski, G. Pastorin, M. Benincasa, C. Klumpp, J. P. Briand, R. Gennaro, M. Prato and A. Bianco, *Angew. Chem., Int. Ed.*, 2005, **44**, 6358.
19 Z. Liu, X. Sun, N. Nakayama-Rathford and H. Dai, *ACS Nano*, 2007, **1**, 50.
20 L. Zhang, J. Xia, Q. Zhao, L. Liu and Z. Zhang, *Small*, 2010, **6**, 537.
21 Z. Liu, J. T. Robinson, X. Sun, N. Nakayama-Rathford and H. Dai, *J. Am. Chem. Soc.*, 2008, **130**, 10876.
22 H. Ali-Boucetta, K. T. Al-Jamal, D. McCarthy, M. Prato, A. Bianco and K. Kostarelos, *Chem. Commun.*, 2008, 459.
23 N. G. Sahoo, H. K. F. Cheng, L. Li, S. H. Chan, Z. Judeh and J. Zhao, *Adv. Funct. Mater.*, 2009, **19**, 3962.
24 N. I. Kovtyukhova, P. J. Ollivier, B. R. Martin, T. E. Mallouk, S. A. Chizhik, E. V. Buzaneva and A. D. Gorchinskiy, *Chem. Mater.*, 1999, **11**, 771.
25 F. Denizot and R. J. Lang, *J. Immunol. Methods*, 1986, **89**, 271.
26 D. T. Vistica, P. Skehan, D. Scudiero, A. Monks, A. Pittman and M. R. Boyds, *Cancer Res.*, 1991, **51**, 2515.
27 A. Magrez, S. Kasas, V. Salicio, N. Pasquier, J. W. Seo, M. Celio, S. Catsicas, B. Schwaller and L. Forro, *Nano Lett.*, 2006, **6**, 1121.
28 D. Cui, F. Tian, C. O. Ozkan, M. Wang and H. Gao, *Toxicol. Lett.*, 2005, **155**, 73.
29 D. Cai, J. M. Mataraza, Z. H. Qin, Z. Huang, J. Huang, T. C. Chiles, D. Carnahan, K. Kempa and Z. Ren, *Nat. Methods*, 2005, **2**, 449–454.
30 N. W. S. Kam, T. C. Jessop, P. A. Wender and H. Dai, *J. Am. Chem. Soc.*, 2004, **126**, 6850.
31 R. Li, R. Wu, L. Zhao, M. Wu, L. Yang and H. Zou, *ACS Nano*, 2010, **4**, 1399.